

EPA's Virtual Embryo

TB Knudsen, PhD
National Center for Computational Toxicology

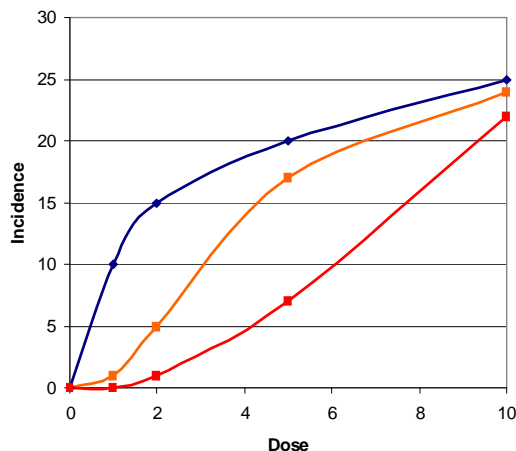
UNITED STATES ENVIRONMENTAL PROTECTION AGENCY



Disclaimer: views are those of the presenter and do not necessarily reflect Agency policy nor imply endorsement of software used here

Developmental toxicity

- ❖ **Endpoint:** adverse effects of chemicals following maternal exposure during pregnancy-lactation
- ❖ **Cause:** disruption of morphogenesis and differentiation via direct (embryonal) or indirect (maternal) chemical targets
- ❖ **Manifestation:** traditionally evaluated in two lab animal species, usually rat and rabbit, monitoring endpoints for:



1. fetal growth retardation (FWR)
2. structural defects (malformations)
3. fetal deaths (resorptions)
4. functional deficits (latent disorders)

Profiling developmental toxicity

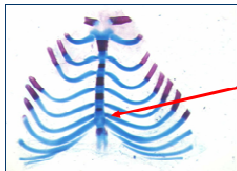
In vivo endpoints (target, description)

www.epa.gov/ncct/toxrefdb

images from www.DevTox.org



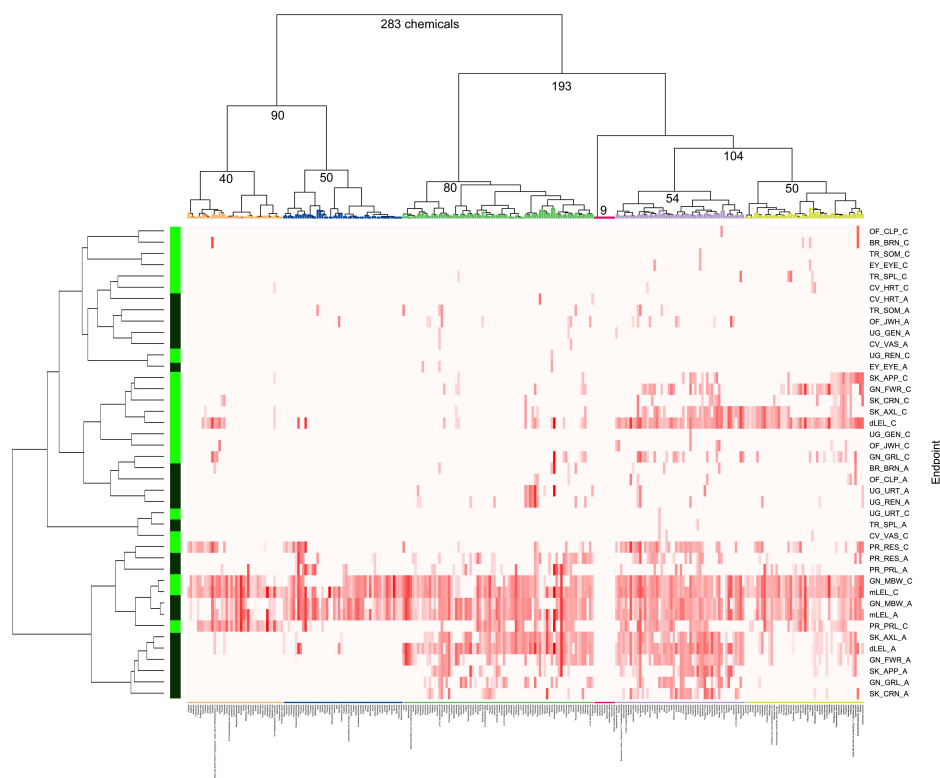
target: kidney
description: absent renal papilla
code: UG_REN_3.1060.5013



target: sternebra
description: incomplete ossification
code: SK_AXL_2.1099.5130



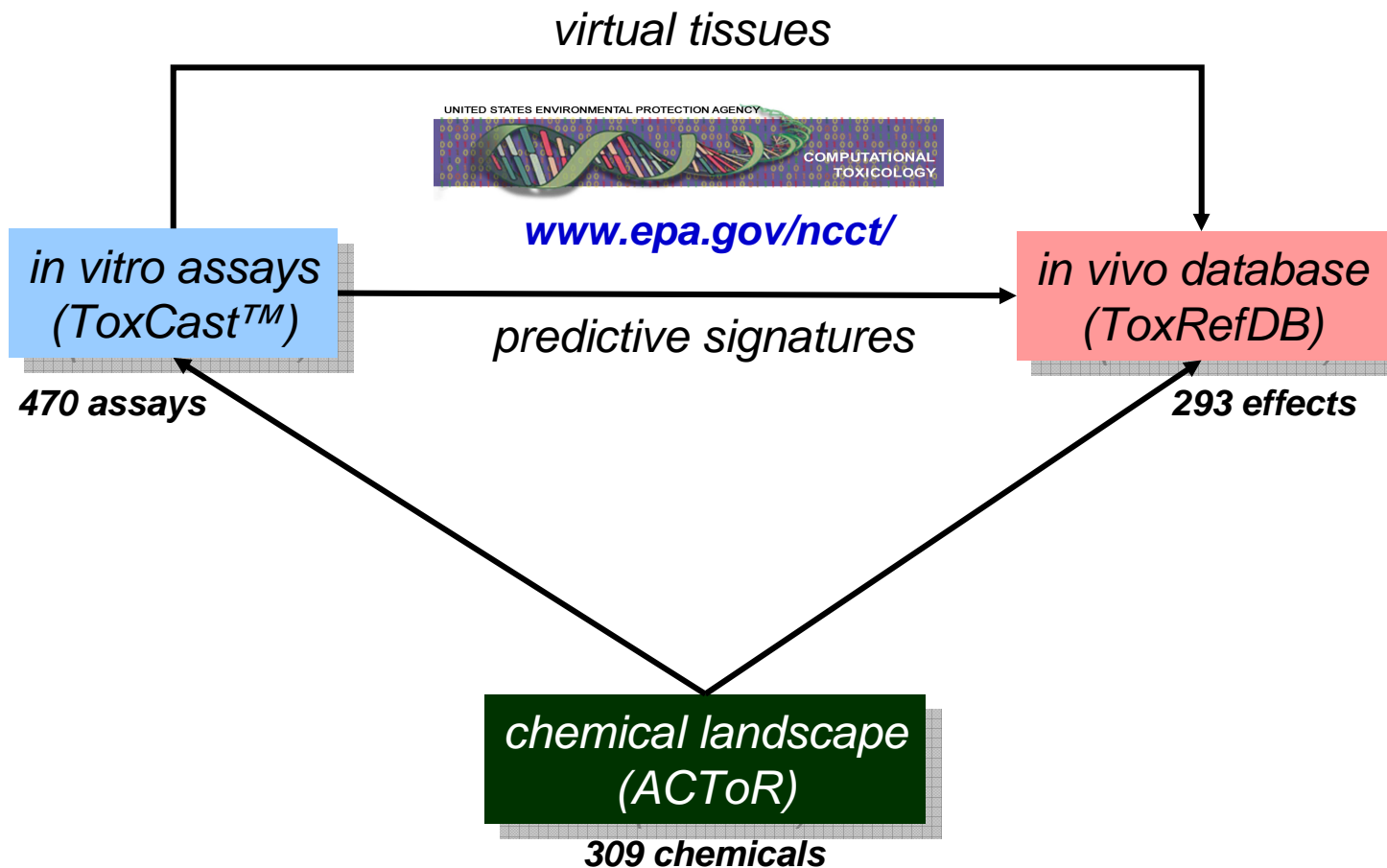
target: hindpaw
description: polydactyly (digit I)
code: SK_APP_2.1051.5234



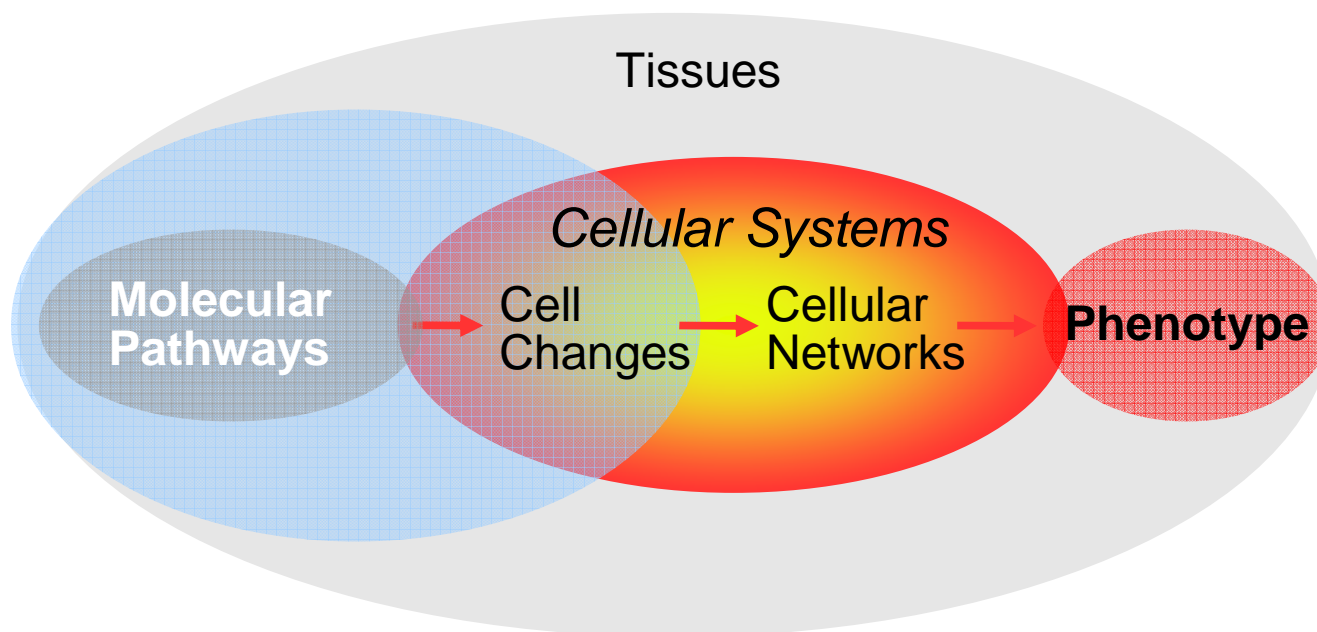
ToxRefDB 387 chemicals, 751 prenatal studies,
988 effects annotated (enhanced DevTox.org)

283 chemicals x 293 effects → 19 target
systems from rat (■) and rabbit (■) studies

Goal: predictive modeling & understanding mechanisms of developmental toxicity



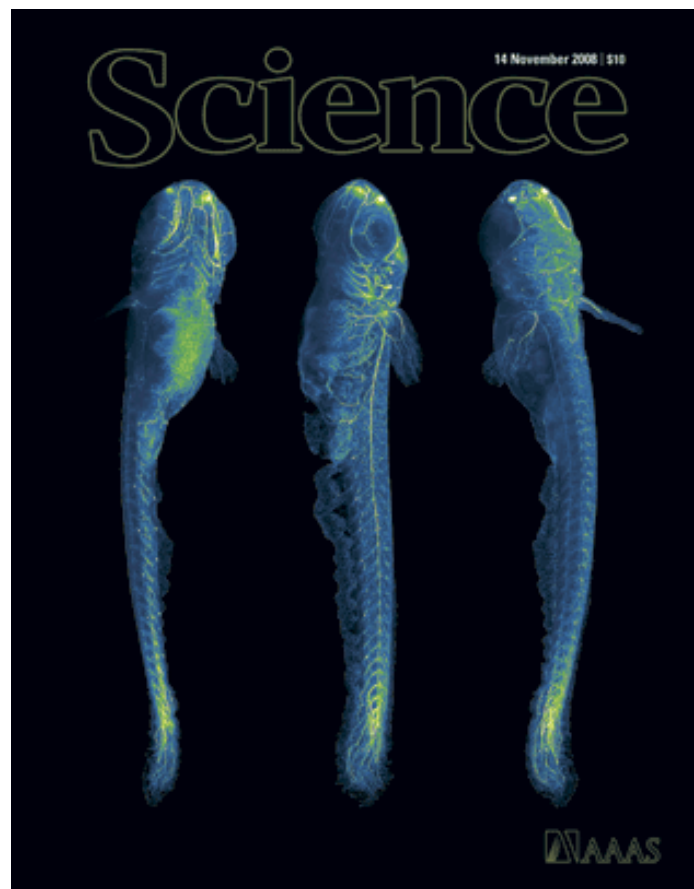
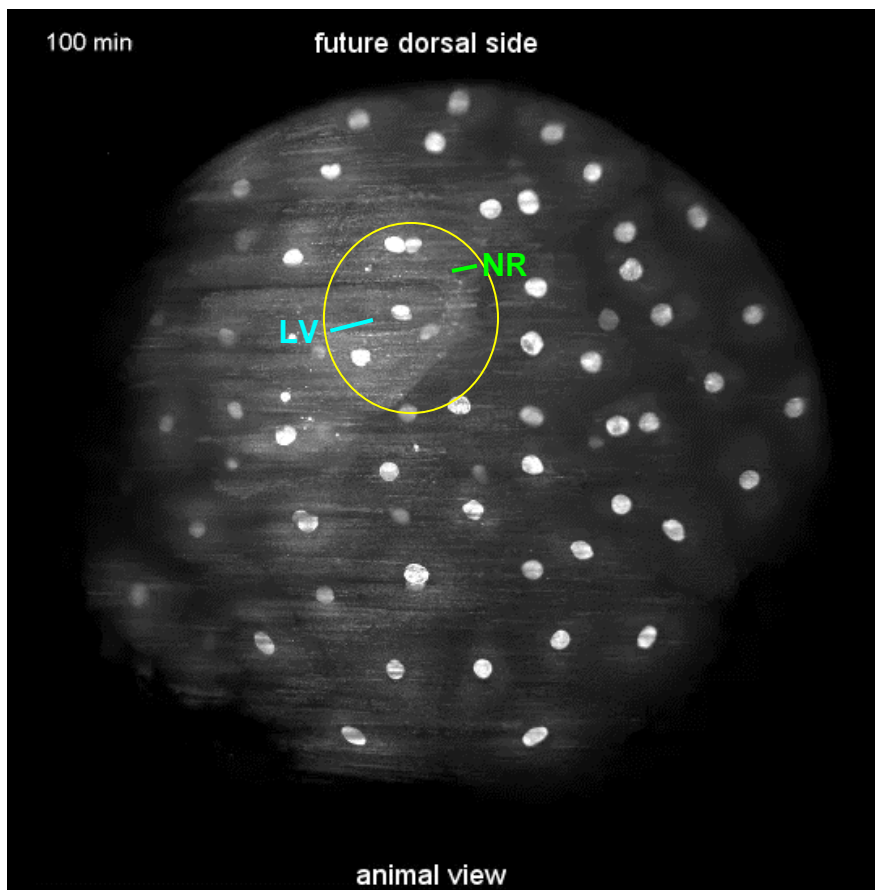
Computational (*in silico*) models



VIRTUAL TISSUES PARADIGM

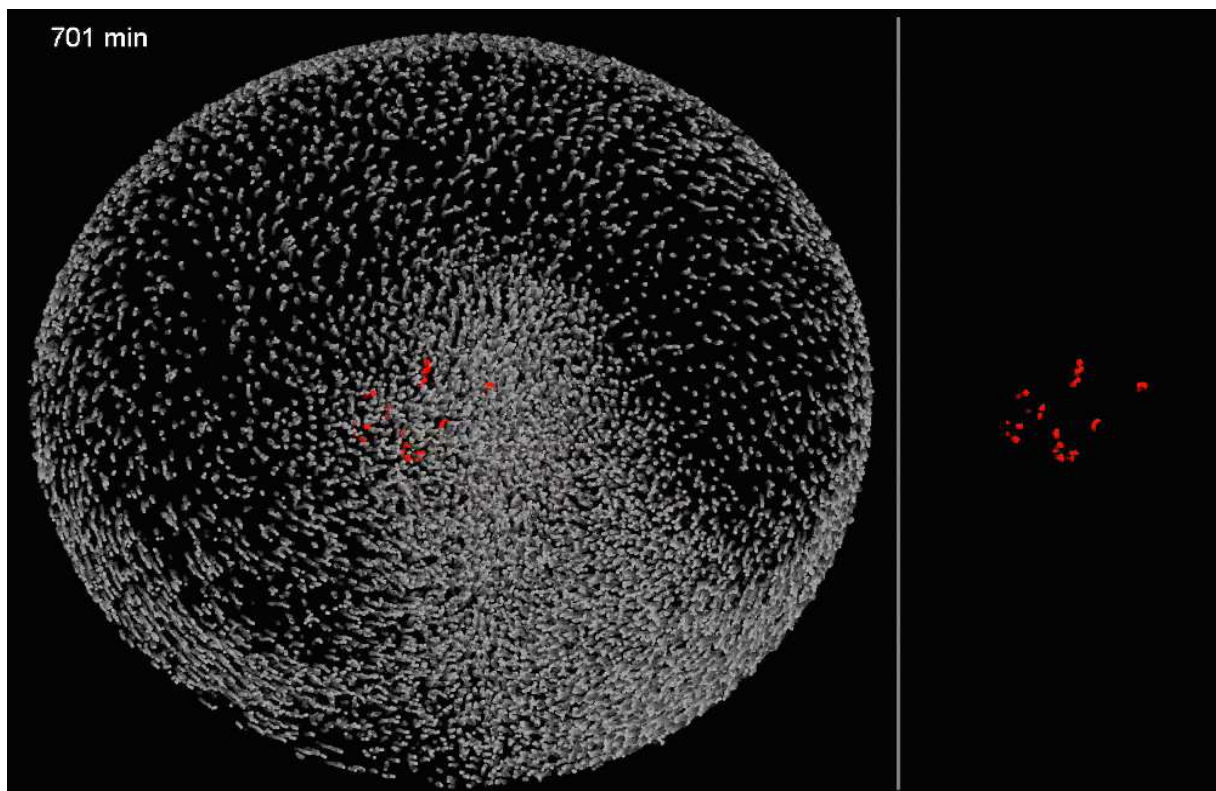
- local cell changes linked to pathway-level perturbation
- then propagated to a higher level by systems of interacting cells
- network state relationships ultimately determine the outcome

Digital embryo: image-based reconstruction of a zebrafish embryo



early embryonic development tracked with H2B-EGFP
by DSLM at 90s intervals over 18h

Morphogenetic blueprint



reverse-engineering the cellular dynamics in
optic vesicle formation

Toolbox of morphogenesis

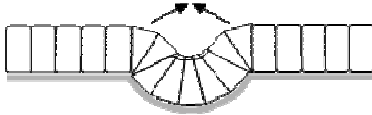

Core developmental processes

- patterning (sets up future events)
- timing (clocks and oscillators)
- differentiation (cell diversification)
- morphogenesis (tissue organization)

Cellular primitives

- growth (proliferation)
- death (apoptosis)
- differentiation (function)
- adhesion (DAH)
- shape (geometry)
- motility (cell migration)
- ECM (remodeling)

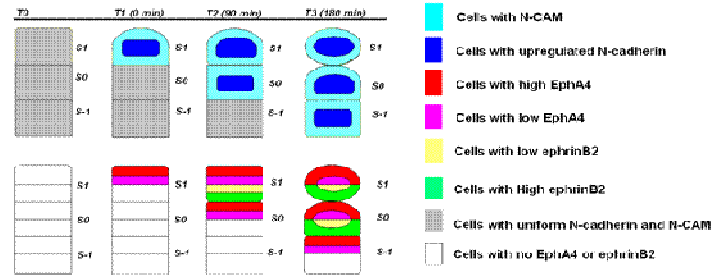
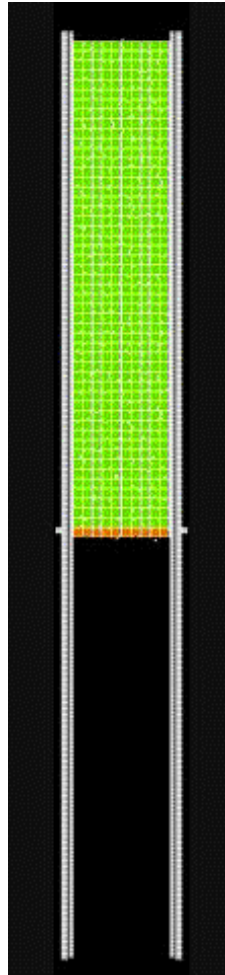
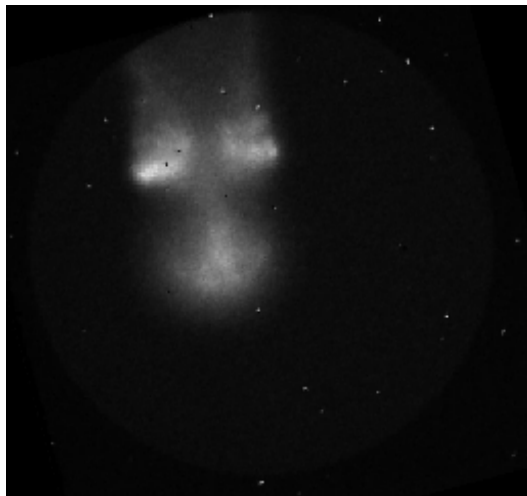
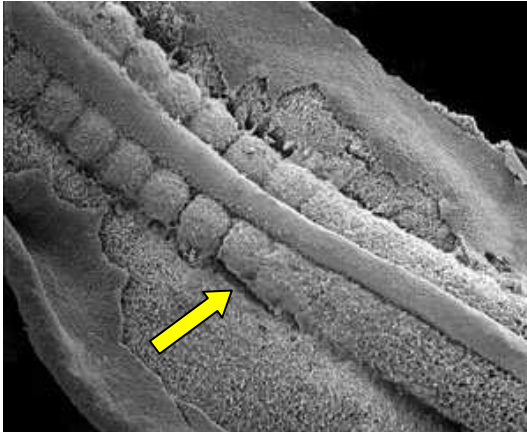
Morphogenetic movement

- folding 
- epiboly
- convergent extension
- branching morphogenesis
- cell condensation
- cell sorting
- trans-differentiation
- cavitation 
- involution
- tractional forces

Directed cell movement

- contact guidance (boundaries)
- haptotaxis (ECM tracks)
- chemotaxis (chemical signals)

'Cells' as autonomous agents: example: somite segmentation clock



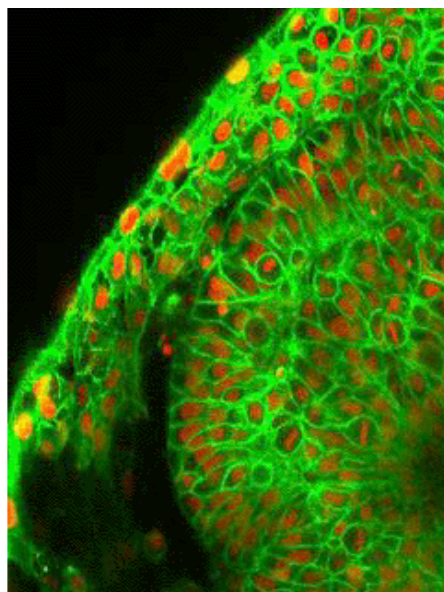
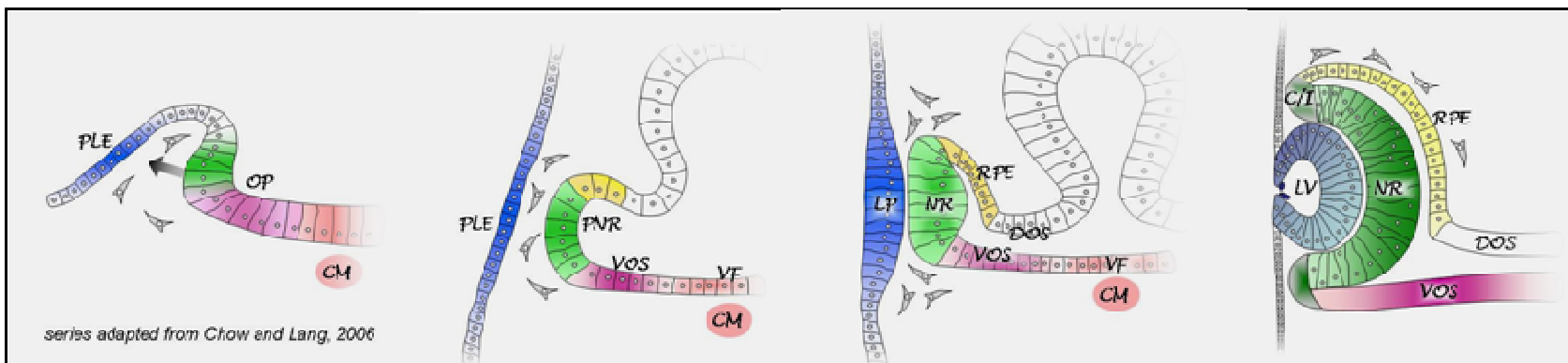
◀ *In silico model, CompuCell3D software*
SOURCE: Glazier et al. (2008) *Cur Top Dev Biol* 81:205



Prenatal exposure, boric acid
SOURCE: John Rogers, RTD/EPA

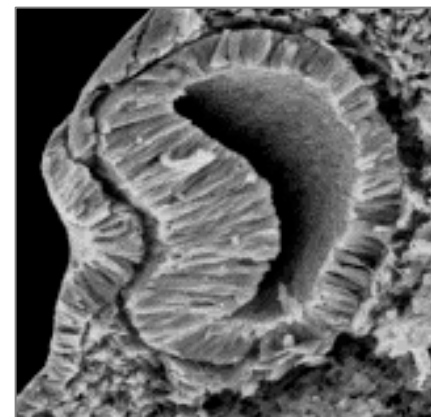
▶ *Hes1-EGFP time-lapse (3h) clock-wavefront*
SOURCE: Masamizu et al. (2006) *PNAS USA* 103:1313-18

Early eye development



**Zebrafish embryo
membrane: EGFP-CAAX
nuclei: H2A.F/Z-mCherry**

◀ **SOURCE: CB Chien lab (2009)**
<http://chien.neuro.utah.edu/>



Mouse embryo ▶
Source: K Sulik
<http://www.med.unc.edu/embryo>

PURPOSE: The *PAX6* gene was first described as a candidate for human aniridia. However, *PAX6* expression is not restricted to the eye and it appears to be crucial for brain development. We studied *PAX6* mutations in a large spectrum of patients who presented with aniridia phenotypes, and anterior segment malformations associated or not with neurological anomalies. **METHODS:** Patients and related families were ophthalmologically phenotyped, and in some cases neurologically and endocrinologically examined. We screened the *PAX6* gene by direct sequencing in three groups of patients: those affected by aniridia, those with diverse ocular manifestations, and those with Petersen's anomaly. Two mutations were investigated by generating crystallographic representations of the amino acid changes. **RESULTS:** Three novel heterozygous mutations affecting three unrelated families were identified: the g.5721>g.c. C nucleotide change, located in exon 5, and corresponding to the Leucine 46 Proline amino-acid mutation (L46P); the g.655A>g.t. G nucleotide change, located in exon 6, and corresponding to the Serine 74 Glycine amino-acid mutation (S74G); and the nucleotide deletion 579delG del, located in exon 6, which induces a frameshift mutation leading to a stop codon (V495fsX3). The L46P mutation was identified in affected patients presenting bilateral microphthalmia, cataracts, and nystagmus. The S74G mutation was found in a large family that had congenital ocular abnormalities, diverse neurological manifestations, and variable cognitive impairments. The 579delG deletion (V495fsX3) caused in the affected members of the same family bilateral aniridia associated with congenital cataract, foveal hypoplasia, and nystagmus. We also detected a novel intronic nucleotide change, IVS2+9G>g.t. A (very likely a mutation) in an apparently isolated patient affected by a complex ocular phenotype, characterized primarily by a bilateral microphthalmia. Whether this nucleotide change is indeed pathogenic remains to be demonstrated. Two previously known heterozygous mutations of the *PAX6* gene sequence were also detected in patients affected by aniridia: a de novo previously known nucleotide change, g.372>C>g.t. T (G178), in exon 6, leading to a stop codon and a heterozygous g.555>g.t. A (C40V) recurrent nonsense mutation in exon 5. No mutations were found in patients with Petersen's anomaly. **CONCLUSIONS:** We identified three mutations associated with aniridia phenotypes (G178X, C40V, and V495fsX3). The three other mutations reported here cause non-aniridia ocular phenotypes associated in some cases with neurological anomalies. The IVS2+9G>g.t. A nucleotide change was detected in a patient with a microphthalmia phenotype. The L46P mutation was detected in a family with microphthalmia, cataract, and nystagmus. This mutation is located in the DNA-binding paired-domain and the crystallographic representations of this mutation show that this mutation may affect the helix-turn-helix motif, and as a consequence the DNA-binding properties of the resulting mutated protein. Ser74 is located in the *PAX6* PD linker region, essential for DNA recognition and DNA binding, and the side chain of the Ser74 contributes to DNA recognition by the linker domain through direct contacts. Crystallographic representations show that the S74G mutation results in no side chain and therefore perturbs the DNA-binding properties of *PAX6*. This study highlights the severity and diversity of the consequences of *PAX6* mutations that appeared to result from the complexity of the *PAX6* gene structure, and the numerous possibilities for DNA binding. This study emphasizes the fact that neurodevelopmental abnormalities may be caused by *PAX6* mutations. The neurodevelopmental abnormalities caused by *PAX6* mutations are probably still overlooked in the current clinical examinations performed throughout the world in patients affected by *PAX6* mutations.

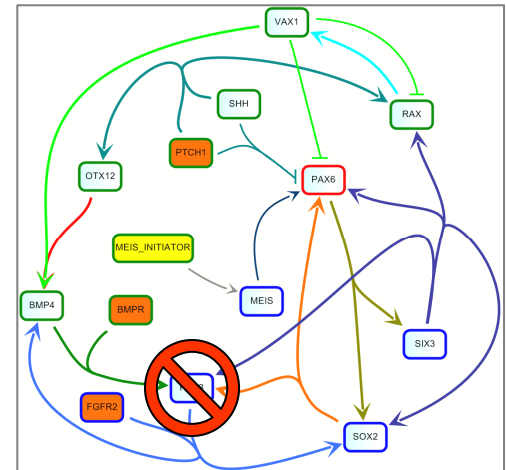
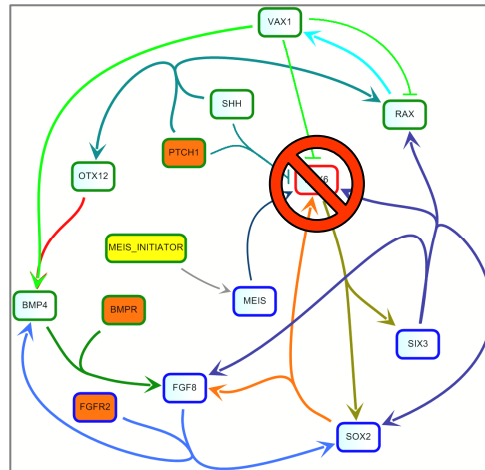
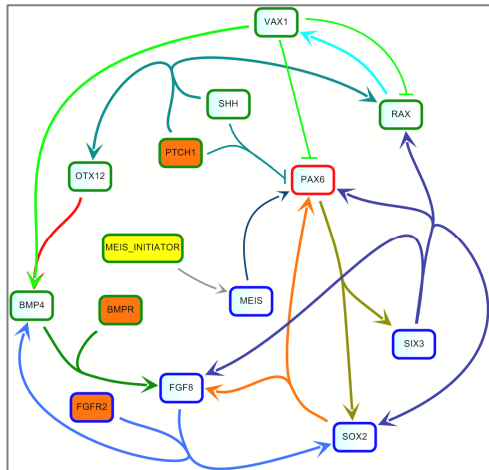
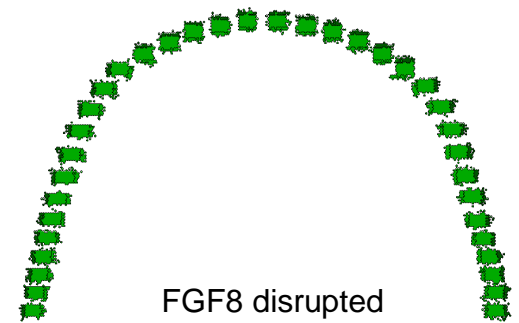
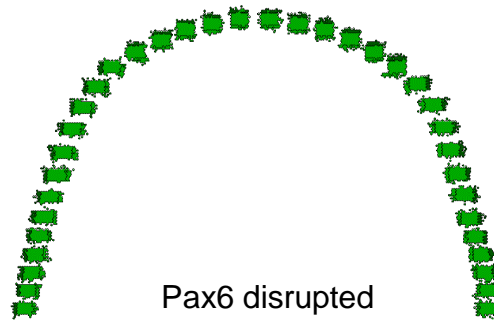
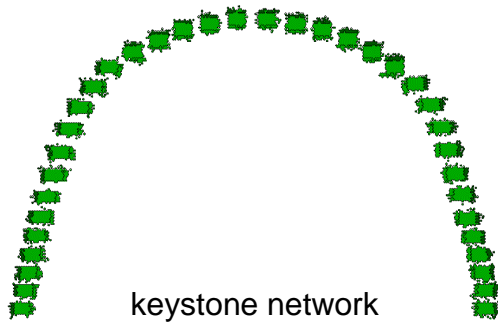
Accession	Species	Gene	Protein	Position	Change	Effect	Source
392	Human	Pax6	Pax6	1008-68-09	T	%	%
393	Human	Pax6	Pax6	1008-68-09	T	%	%
394	Human	Pax6	Pax6	1008-68-09	T	%	%
395	Human	Pax6	Pax6	1008-68-09	T	%	%
396	Human	Pax6	Pax6	1008-68-09	T	%	%
397	Human	Pax6	Pax6	1008-68-09	T	%	%
398	Human	Pax6	Pax6	1008-68-09	T	%	%
399	Human	Pax6	Pax6	1008-68-09	T	%	%
400	Human	Pax6	Pax6	1008-68-09	T	%	%
401	Human	Pax6	Pax6	1008-68-09	T	%	%
402	Human	Pax6	Pax6	1008-68-09	T	%	%
403	Human	Pax6	Pax6	1008-68-09	T	%	%
404	Human	Pax6	Pax6	1008-68-09	T	%	%
405	Human	Pax6	Pax6	1008-68-09	T	%	%
406	Human	Pax6	Pax6	1008-68-09	T	%	%
407	Human	Pax6	Pax6	1008-68-09	T	%	%
408	Human	Pax6	Pax6	1008-68-09	T	%	%
409	Human	Pax6	Pax6	1008-68-09	T	%	%
410	Human	Pax6	Pax6	1008-68-09	T	%	%
411	Human	Pax6	Pax6	1008-68-09	T	%	%
412	Human	Pax6	Pax6	1008-68-09	T	%	%
413	Human	Pax6	Pax6	1008-68-09	T	%	%
414	Human	Pax6	Pax6	1008-68-09	T	%	%
415	Human	Pax6	Pax6	1008-68-09	T	%	%
416	Human	Pax6	Pax6	1008-68-09	T	%	%
417	Human	Pax6	Pax6	1008-68-09	T	%	%
418	Human	Pax6	Pax6	1008-68-09	T	%	%
419	Human	Pax6	Pax6	1008-68-09	T	%	%
420	Human	Pax6	Pax6	1008-68-09	T	%	%
421	Human	Pax6	Pax6	1008-68-09	T	%	%
422	Human	Pax6	Pax6	1008-68-09	T	%	%
423	Human	Pax6	Pax6	1008-68-09	T	%	%
424	Human	Pax6	Pax6	1008-68-09	T	%	%
425	Human	Pax6	Pax6	1008-68-09	T	%	%
426	Human	Pax6	Pax6	1008-68-09	T	%	%
427	Human	Pax6	Pax6	1008-68-09	T	%	%
428	Human	Pax6	Pax6	1008-68-09	T	%	%
429	Human	Pax6	Pax6	1008-68-09	T	%	%
430	Human	Pax6	Pax6	1008-68-09	T	%	%
431	Human	Pax6	Pax6	1008-68-09	T	%	%
432	Human	Pax6	Pax6	1008-68-09	T	%	%
433	Human	Pax6	Pax6	1008-68-09	T	%	%
434	Human	Pax6	Pax6	1008-68-09	T	%	%
435	Human	Pax6	Pax6	1008-68-09	T	%	%
436	Human	Pax6	Pax6	1008-68-09	T	%	%
437	Human	Pax6	Pax6	1008-68-09	T	%	%
438	Human	Pax6	Pax6	1008-68-09	T	%	%
439	Human	Pax6	Pax6	1008-68-09	T	%	%
440	Human	Pax6	Pax6	1008-68-09	T	%	%
441	Human	Pax6	Pax6	1008-68-09	T	%	%
442	Human	Pax6	Pax6	1008-68-09	T	%	%
443	Human	Pax6	Pax6	1008-68-09	T	%	%
444	Human	Pax6	Pax6	1008-68-09	T	%	%
445	Human	Pax6	Pax6	1008-68-09	T	%	%
446	Human	Pax6	Pax6	1008-68-09	T	%	%
447	Human	Pax6	Pax6	1008-68-09	T	%	%
448	Human	Pax6	Pax6	1008-68-09	T	%	%
449	Human	Pax6	Pax6	1008-68-09	T	%	%
450	Human	Pax6	Pax6	1008-68-09	T	%	%
451	Human	Pax6	Pax6	1008-68-09	T	%	%
452	Human	Pax6	Pax6	1008-68-09	T	%	%
453	Human	Pax6	Pax6	1008-68-09	T	%	%
454	Human	Pax6	Pax6	1008-68-09	T	%	%
455	Human	Pax6	Pax6	1008-68-09	T	%	%
456	Human	Pax6	Pax6	1008-68-09	T	%	%
457	Human	Pax6	Pax6	1008-68-09	T	%	%
458	Human	Pax6	Pax6	1008-68-09	T	%	%
459	Human	Pax6	Pax6	1008-68-09	T	%	%
460	Human	Pax6	Pax6	1008-68-09	T	%	%
461	Human	Pax6	Pax6	1008-68-09	T	%	%
462	Human	Pax6	Pax6	1008-68-09	T	%	%
463	Human	Pax6	Pax6	1008-68-09	T	%	%
464	Human	Pax6	Pax6	1008-68-09	T	%	%
465	Human	Pax6	Pax6	1008-68-09	T	%	%
466	Human	Pax6	Pax6	1008-68-09	T	%	%
467	Human	Pax6	Pax6	1008-68-09	T	%	%
468	Human	Pax6	Pax6	1008-68-09	T	%	%
469	Human	Pax6	Pax6	1008-68-09	T	%	%
470	Human	Pax6	Pax6	1008-68-09	T	%	%
471	Human	Pax6	Pax6	1008-68-09	T	%	%
472	Human	Pax6	Pax6	1008-68-09	T	%	%
473	Human	Pax6	Pax6	1008-68-09	T	%	%
474	Human	Pax6	Pax6	1008-68-09	T	%	%
475	Human	Pax6	Pax6	1008-68-09	T	%	%
476	Human	Pax6	Pax6	1008-68-09	T	%	%
477	Human	Pax6	Pax6	1008-68-09	T	%	%
478	Human	Pax6	Pax6	1008-68-09	T	%	%
479	Human	Pax6	Pax6	1008-68-09	T	%	%
480	Human	Pax6	Pax6	1008-68-09	T	%	%
481	Human	Pax6	Pax6	1008-68-09	T	%	%
482	Human	Pax6	Pax6	1008-68-09	T	%	%
483	Human	Pax6	Pax6	1008-68-09	T	%	%
484	Human	Pax6	Pax6	1008-68-09	T	%	%
485	Human	Pax6	Pax6	1008-68-09	T	%	%
486	Human	Pax6	Pax6	1008-68-09	T	%	%
487	Human	Pax6	Pax6	1008-68-09	T	%	%
488	Human	Pax6	Pax6	1008-68-09	T	%	%
489	Human	Pax6	Pax6	1008-68-09	T	%	%
490	Human	Pax6	Pax6	1008-68-09	T	%	%
491	Human	Pax6	Pax6	1008-68-09	T	%	%
492	Human	Pax6	Pax6	1008-68-09	T	%	%
493	Human	Pax6	Pax6	1008-68-09	T	%	%
494	Human	Pax6	Pax6	1008-68-09	T	%	%
495	Human	Pax6	Pax6	1008-68-09	T	%	%
496	Human	Pax6	Pax6	1008-68-09	T	%	%
497	Human	Pax6	Pax6	1008-68-09	T	%	%
498	Human	Pax6	Pax6	1008-68-09	T	%	%
499	Human	Pax6	Pax6	1008-68-09	T	%	%
500	Human	Pax6	Pax6	1008-68-09	T	%	%

EMAGI	DevTox	Pa	Pb	Pab	Sscore	Rscore
Wnt2b	Microphthalmia	38	365	1	3.065753	0.486537
Vax1	Ocular coloboma	11	120	3	96.64091	1.985161
Tbx3	Microphthalmia	47	365	1	2.478694	0.394223
Tbx2	Microphthalmia	55	365	1	2.118157	0.325958
Sox2	Anophthalmia	221	193	3	2.990786	0.475785
Sox2	Ocular coloboma	221	120	1	1.603394	0.20504
Sox2	Small lens	221	103	1	1.868031	0.271384
Six6	Anophthalmia	23	193	2	19.15837	1.282359
Six6	Microphthalmia	23	365	1	5.065158	0.704593
Six6	Retina fold	23	88	1	21.00889	1.322403
Six3	Anophthalmia	94	193	4	9.375372	0.971989
Six3	Microphthalmia	94	365	5	6.196736	0.792163
Six3	Ocular coloboma	94	120	1	3.769681	0.576305
Six3	Open eye	94	153	1	2.956612	0.470794
Six3	Retina fold	94	88	1	5.140474	0.711003
Six3	Small lens	94	103	1	4.391861	0.642649
Si	Small lens	444	103	1	0.929808	-0.03161
Rax	Anophthalmia	15	193	1	14.68808	1.166965
Rax	Ocular coloboma	15	120	1	23.62333	1.373341
Rax	Retina fold	15	88	1	32.21364	1.50804
Pax6	Anophthalmia	587	193	2	0.750669	-0.12455
Pax6	Microphthalmia	587	365	11	2.183109	0.339075
Pax6	Ocular coloboma	587	120	5	3.018313	0.479764
Pax6	Open eye	587	153	2	0.946922	-0.02369
Pax6	Small lens	587	103	10	7.032963	0.847138
Pax2	Aphakia	335	29	1	4.376943	0.641171
Pax2	Microphthalmia	335	365	1	0.347757	-0.45872
Pax2	Ocular coloboma	335	120	16	16.92418	1.228508
Otx2	Anophthalmia	239	193	1	0.921846	-0.03534
Otx2	Microphthalmia	239	365	2	0.974884	-0.01105
Otx2	Open eye	239	153	1	1.162852	0.065524
Msx2	Microphthalmia	200	365	1	0.582493	-0.23471
Mitf	Microphthalmia	100	365	42	48.92942	1.68957
Mitf	Retina fold	100	88	1	4.832045	0.684131
Meis1	Microphthalmia	42	365	1	2.773777	0.443072
Bmp4	Anophthalmia	518	193	1	0.425331	-0.37127
Bmp4	Microphthalmia	518	365	2	0.449802	-0.34698

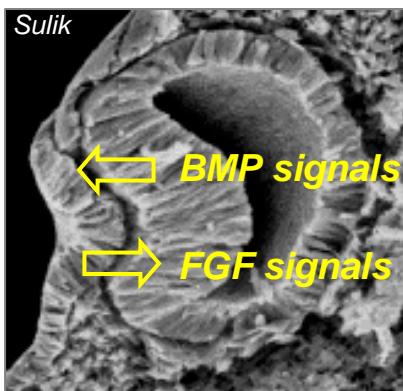
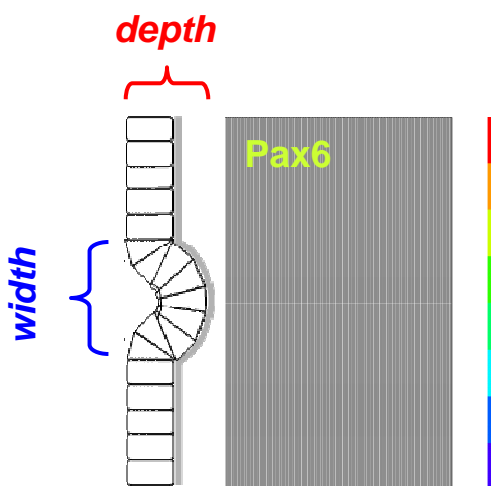
TM PubMed returned 5,889 records for ocular genes in development across 4 species (rat, mouse, zebrafish, human)

Computing relevance scores for association of gene-malformation in the eye based on co-occurrence of DevTox terms in the abstracts

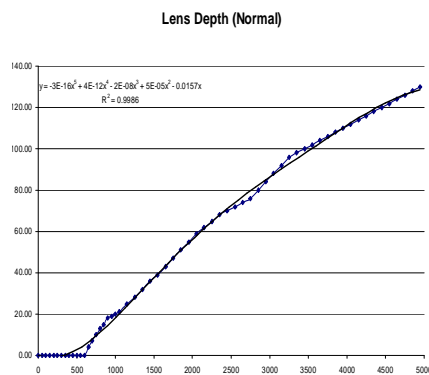
CC3D arrays



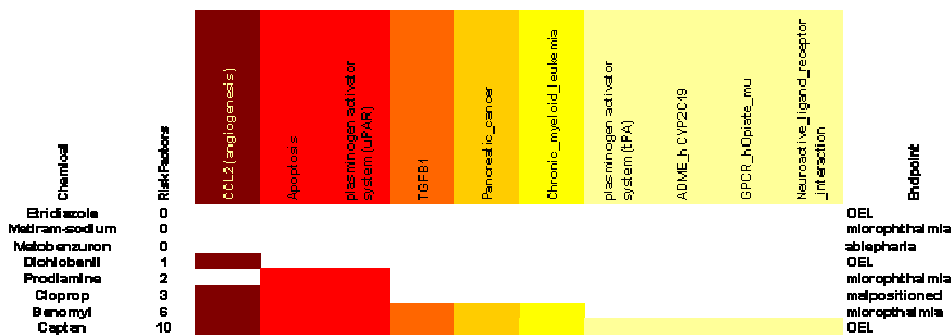
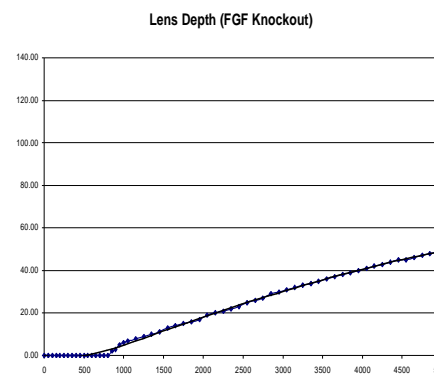
Developmental trajectory of lens: ToxCast™ module predicting eye defects



network enabled



FGF8 disrupted



- plasminogen activating system**
- ECM remodeling in angiogenesis
 - TGF-beta family activation
 - mobilization of FGF signals

EPA's Virtual Embryo



- ❖ **Motivation:** computational models to navigate complex relationships in the embryo and predict key *in vivo* events from *in vitro* data
- ❖ **Research goal:** simulate embryonic tissues reacting to perturbation across chemical class, system, stage, genetic makeup, dose and time
- ❖ **Inputs:** detailed knowledge of biochemical targets, molecular pathways, cellular networks, and emergent phenotypes
- ❖ **Outputs:** modular reconstruction of specific systems (short-term) and the human embryo (long-term)

Acknowledgements

<http://www.epa.gov/ncct/v-Embryo/>



Virtual Embryo

Amar Singh

Michael Rountree

Richard Spencer

NHEERL

Sid Hunter

Stephanie Padilla



Virtual Tissues

Imran Shah

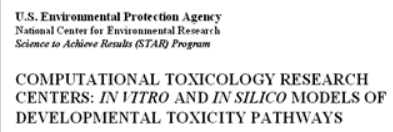
Rory Conolly

John Wambaugh

Woody Setzer

Jason Pirone

Pending



ToxCast

Matt Martin

David Dix

Bob Kavlock

Richard Judson

Keith Houck

